



MINISTRY OF TECHNOLOGY
AERONAUTICAL RESEARCH COUNCIL
CURRENT PAPERS

Delta Wings with Longitudinal Camber at Low Speed

By
R. K. Nangia and G. J. Hancock,
Dept. of Aeronautical Engineering,
Queen Mary College, University of London

LONDON HER MAJESTY'S STATIONERY OFFICE

1970

PRICE 7s 6d [37½p] NET

Delta Wings with Longitudinal
Camber at Low Speed

- By -

R. K. Nangia and G. J. Hancock,
Dept. of Aeronautical Engineering,
Queen Mary College, University of London

SUMMARY

Experiments on a delta wing of aspect ratio 1 with various streamwise cambers are reported. Comparison of experimental results for the streamwise lift distribution with Taylor's simplified slender linear theory is remarkably good even for large cambers, although linear theory is totally inadequate for total lift prediction. The good agreement between experiment and linear theory for the streamwise lift distribution indicates support for the recent intuitive ideas of Polhamus.

List of Contents

	<u>Page</u>
Summary	1
Contents	1
I. <u>Introduction</u>	2
II. <u>Experimental Programme</u>	2
II.1 Smoke Visualisation Tests	3
II.2 Pressure Plotting Models	3
II.3 Surface Streamline Flow Visualisation	3
III. <u>Results</u>	4
III.1 Smoke Tests	4
III.2 Surface Streamline Patterns	4
III.3 Pressure Distributions	5
III.4 Longitudinal Lift Distribution	6
IV. <u>Comparison With Linear Theory</u>	6
V. <u>Concluding Remarks</u>	7
References	8

I. Introduction

Aeroelasticity of slender wings has been of considerable interest over the past few years. In particular, Hancock⁽¹⁾ and Milne⁽²⁾ have been concerned with the development of theoretical methods dealing with the longitudinal deformation effects in flight of slender wings which were regarded structurally as 'beam like'. To develop these methods further more fundamental quantitative aerodynamic information is required on the longitudinal distribution of lift due to longitudinal camber.

A programme of research⁽³⁾ was undertaken to investigate the aerodynamics of the low speed flow about delta wings with longitudinal camber. In this note some of the experimental results are reported. Other theoretical work concerned with development of non-linear theory to predict the lift distribution over a delta wing at low speeds incorporating the Kutta trailing edge condition is published elsewhere⁽⁴⁾.

The experimental work included in this note covers results from flow visualisation tests, using smoke to show the leading edge vortices and 'day-glo' techniques for surface patterns, and measured pressure distributions on a delta wing of aspect ratio 1 with different longitudinal cambers. To obtain a range of these longitudinal cambers without the manufacture of many models, a technique was used of successively 'suction-moulding', after heating, a perspex wing to a series of desired camber shapes. This technique is based on the previous work of Black⁽⁵⁾ on more conventional swept wings.

One of the surprising features to emerge from the present investigation was that the simplified slender linear theory of Taylor⁽⁶⁾ predicts the shape of the chordwise load distribution on flat and chordwise cambered wings with good accuracy even when the camber is large in spite of the fact that linear theory gives values of total lift far lower than the practical values.

The excellent agreement between experiment and linear theory for the chordwise lift distribution seems to indicate support for the recent ideas of Polhamus⁽⁷⁾. Polhamus argues that linear theory can be used to predict the non linear lift on a wing with leading edge separation if the linear leading edge suction force is rotated through a right angle normal to the wing surface to give the additional non linear lift increment. On slender wings one might expect that the lengthwise distribution of the linearised leading edge suction force would be similar to the lengthwise linearised lift distribution, thus according to Polhamus the non-linear lift distribution would then be similar to the linear distribution.

II. Experimental Programme

The experimental programme was concerned with the investigation of the steady flow characteristics about a delta wing with longitudinal (or chordwise, or streamwise, or lengthwise) camber. Qualitative aspects were obtained by flow visualisation of leading edge vortex paths using smoke, together with studies of the surface streamline flow patterns. Extensive pressure plotting of a delta wing of unit aspect ratio with and without longitudinal camber gave more quantitative data.

II.1 Smoke Visualisation Tests

A number of models, all of root chord 9 ins, were constructed from 1/8 inch thick dural sheeting; the leading edges were chamfered at an angle of 45° . Three low aspect ratios (0.5, 0.75, 1.0) and a range of circular cambers (up to 0.1) were covered. The camber λ is defined as the ratio of maximum height of wing measured from the plane forming the apex to the wing tips to the root chord of the wing.

Smoke was generated by heating 'soldering resin flux' over a small electrical element set flush in the surface of the model near the apex.

These models were tested in a small return circuit wind tunnel of working section 10.5 inches square at speeds of 10-15 ft/sec..

II.2 Pressure Plotting Models

Model wings of unit aspect ratio and thickness/root chord ratio 0.0209 were constructed from perspex with pressure tubings along conical rays from the apex on both surfaces. The leading edge shape was symmetric, featuring bevelled edges at right angles. Pressures could be recorded at up to 13 points in spanwise direction on each of the two surfaces at up to 16 chordwise stations.

Different cambers were obtained by first heating the model in an oven and then cooling while held in a vacuum mould, the apparatus is shown in Fig 1. Separate moulds were required for each camber.

Two uncambered wings of chord length 24" and 12" respectively were made. Most of the pressure plotting was carried out on the larger wing; the smaller wing was used to check out scale effects, tunnel interference, etc. Only the results for the larger wing are given in this note.

The larger wing (designated A) was moulded into a 3.57% cambered wing (designated B) and a 9.46% cambered wing (designated C). The camber shapes are shown in Fig 2. The original intention was to achieve circular cambers of 5% and 10% respectively for wings B and C but due to 'relaxing' in the material, after cooling, neither of these values, nor indeed the true circular shape was subsequently attained.

All wings were pressure plotted at an airspeed of 90 ft/sec in a blow-down wind tunnel of working section of height 39" and width 30". The models were sting mounted at the centre of tunnel; both positive and negative attitudes of the model were investigated. At extreme attitudes the wing apex was close to the ceiling (or floor) of the tunnel working section; errors due to this effect have not been taken out of the results presented in this note. Detailed comparisons of the pressure distributions between the larger and smaller wings show that these errors are not serious enough to invalidate the conclusions in this note, the complete data is presented in ref 3.

II.3 Surface Streamline Flow Visualisation

The well established 'day-glo' technique was employed on the pressure plotting models after covering the exterior surfaces with a special type of paper with a smooth plasticated surface (commercially

known as 'Fablon') to protect the pressure holes from becoming blocked during the course of experiments.

III. Results

III.1 Smoke Tests

For wings with small, or no camber, the smoke was convected along the line of the leading edge vortex core which was easily definable. With increasing camber the smoke appeared to diffuse into spirals of appreciable diameter; consequently the measurements of vortex position was more difficult. This diffusion was thought not to be related to vortex breakdown. Trends in the spanwise position of the vortex at the trailing edge of flat and cambered wings with nominal incidence are:

- (i) the vortices move inboard with increasing incidence at low incidence, but then tend to remain at a constant spanwise station with further increases of incidence, this stationary process begins at higher angles of incidence as the aspect ratio increases; inward movement is associated with movement upwards away from the wing surface.
- (ii) increasing the aspect ratio for a fixed (positive) camber moves the vortices outboard.
- (iii) increasing the camber for a fixed aspect ratio and fixed mean incidence moves the vortices outboard.

III.2 Surface Streamline Patterns

Surface streamline flow patterns on uncambered delta wings are now well recognised with the upper surface attachment lines, lines of secondary separation, and the familiar herring bone pattern inboard of the primary separation vortex. On the lower surface the flow is attached at all incidences and is mainly streamwise except for the region near to the leading edge, with increasing incidence the edge spanwise flows become larger.

To demonstrate the effect of chordwise camber the surface streamline patterns on wing C (camber 9.46%) are shown in this note; the camber is somewhat extreme but its exaggeration high-lights the flow changes. The patterns are sketched in Fig 3 through a range of positive and negative angles of attack.

At the larger negative incidences the wing behaves as a negatively cambered wing whilst at the normal and positive incidences it behaves as a positively cambered wing. The distinction between upper and lower, or suction and compression, surfaces is not clearly defined and it is more convenient to refer to the surfaces simply as convex and concave.

It is seen from Fig 2 that the difference in local incidence at

the apex and at the trailing edge is of the order of 35° . Therefore in most of the incidence range the front part of the wing is operating in a different flow regime to that at the trailing edge, so the lift in the apex region can be opposite in sign to that in the trailing edge region.

At $\alpha_N = -10^\circ$ the incidence over most of the wing is of the same sign: the flow pattern on the concave surface is somewhat similar to the pattern on the 'suction' surface on a flat wing, on the convex surface the effect of spanwise cross flow is seen to be stronger near the apex than in the trailing edge region because of the large change in local incidences. As the nominal incidence is increased to 0° the main vortex, on the concave surface, bends outwards near the trailing edge region, whilst on the convex surface in the aft half wing attached flow, as in the vicinity of a swept leading edge on a conventional wing, is shown. As α_N is further increased to 10° the main vortex on the concave surface is seen to cross the leading edge forward of the trailing edge, appearing on the convex surface in the region of the wing tip. Increasing α_N further to 20° , and then to 30° , the main vortex crosses the leading edge from the concave to convex surface progressively towards the wing apex. The convex surface shows a pattern due to the interference of two vortex sheets of similar sign merging into one overall pattern. The reasons for two vortex sheets are not clear but it seems that the first of these vortex sheets appears when the local incidence becomes positive followed by a second vortex sheet which corresponds approximately to the crossing point of spiral vortex sheet from the concave surface.

III.3 Pressure Distributions

Complete pressure distributions have been measured over the range of attitudes.

For the flat uncambered wing pressure distributions at the representative chordwise stations $x/c = 0.33$ and 0.83 are shown in Fig 4; a diagrammatic 3D representation of the overall load distribution is shown in Fig 5. These results tie in with those well established in the literature.

For the moderate camber wing B the pressure distributions at the same chordwise stations 0.33 and 0.83 are shown in Fig 6; the diagrammatic 3D representation is shown in Fig 7. Pressure distributions on the highly cambered wing C are shown in Figs 8,9.

It is seen on wing C that there is overall agreement between the pressure distributions and surface flow patterns; where two upper surface vortex systems appear on the convex side at higher positive attitudes there are two corresponding suction peaks; where these two vortex systems merge towards the trailing edge there is only one suction peak. Vortex breakdown is probably occurring on wing C at the 30° angle of attack since the rate of suction increase has decreased and the suction peak is more flattened.

III.4 Longitudinal Lift Distribution

The local normal force coefficient $C_{N_L}(x/c)$ is defined as

$$C_{N_L}(x/c) = \frac{x}{c} \int_{-1}^{+1} \Delta c_p \left(\frac{x}{c}, \frac{y}{kx} \right) d(y/kx)$$

and the total normal force coefficient is

$$C_N = \int_0^1 C_{N_L}(x/c) \cos \left(\tan^{-1} \frac{dz_w(x)}{dx} \right) d(x/c)$$

The local lift coefficient C_{L_L} and the total C_L can be derived by appropriate integration of the resolution of C_{N_L} in direction normal to the flow.

The distributions of C_{N_L} on wings A, B, C are shown in Fig 10.

Variation of total lift coefficient for all these wings is shown in Fig 11. It is of interest to note that for wing B, with the smaller camber, at low incidences there is a tendency for C_L to be slightly larger than C_L for the flat plate wing A at the same nominal incidence, thus conforming with the usual trends, but at higher incidences the non-linear effects act in such a manner as to reduce C_L for wing B relative to wing A. These non-linear effects completely dominate the characteristics of wing C throughout its incidence range, even at small incidences C_L lies below the flat plate $C_L \sim \alpha$ curve.

The lift distributions C_{L_L} for various values of overall C_L for the flat wing A are shown in Fig 12. These show the forward movement of the centre of pressure with increasing C_L .

The lift distributions for the positive and negative camber modes of wings B and C at various lift coefficients are shown in Fig 13.

IV. Comparison With Linear Theory

Taylor⁽⁶⁾ has investigated the load distribution on low aspect ratio wings by assuming that the overall spanwise load distribution is elliptic and determines the chordwise lift distribution from the standard linearised lifting surface equation by satisfying the downwash conditions of points along the centre line.

Taylor's theory has been programmed to obtain both the chordwise lift distribution and the total lift, given the local chordwise incidence distribution on the wing. For the present application, because of the large cambers, the local incidence has been specified at 20 equidistant points along the chord.

As already shown in Fig 11 the linear $C_L \sim \alpha$ curve, according to Taylor's theory, is far below the experimental non-linear curves.

For the chordwise load distribution the linear theory of Taylor provides only one shape for the flat wing A throughout its entire incidence range whereas the non-linear experimental shapes vary with incidence as shown in Fig 12. Experimental and theoretical chordwise lift distributions for flat wing A at various incidences are shown in Fig 14.

Further comparisons of experimental results with linear theory for the case of 3.57% cambered Wing-B and the 9.46% cambered Wing-C are shown in Figs 15 and 16 for various nominal incidences. The agreement is remarkable in all cases including the very extreme case of 9.46% cambered Wing-C at nominal incidence of -4° where the loading has changed sign twice.

As mentioned earlier, the experimental results have not been corrected for any wind tunnel constraint effects; this factor may introduce errors but it is thought that these are not of sufficient magnitude to affect the conclusions in this note.

V. Concluding Remarks

Experimental results have been obtained on a delta wing with streamwise camber.

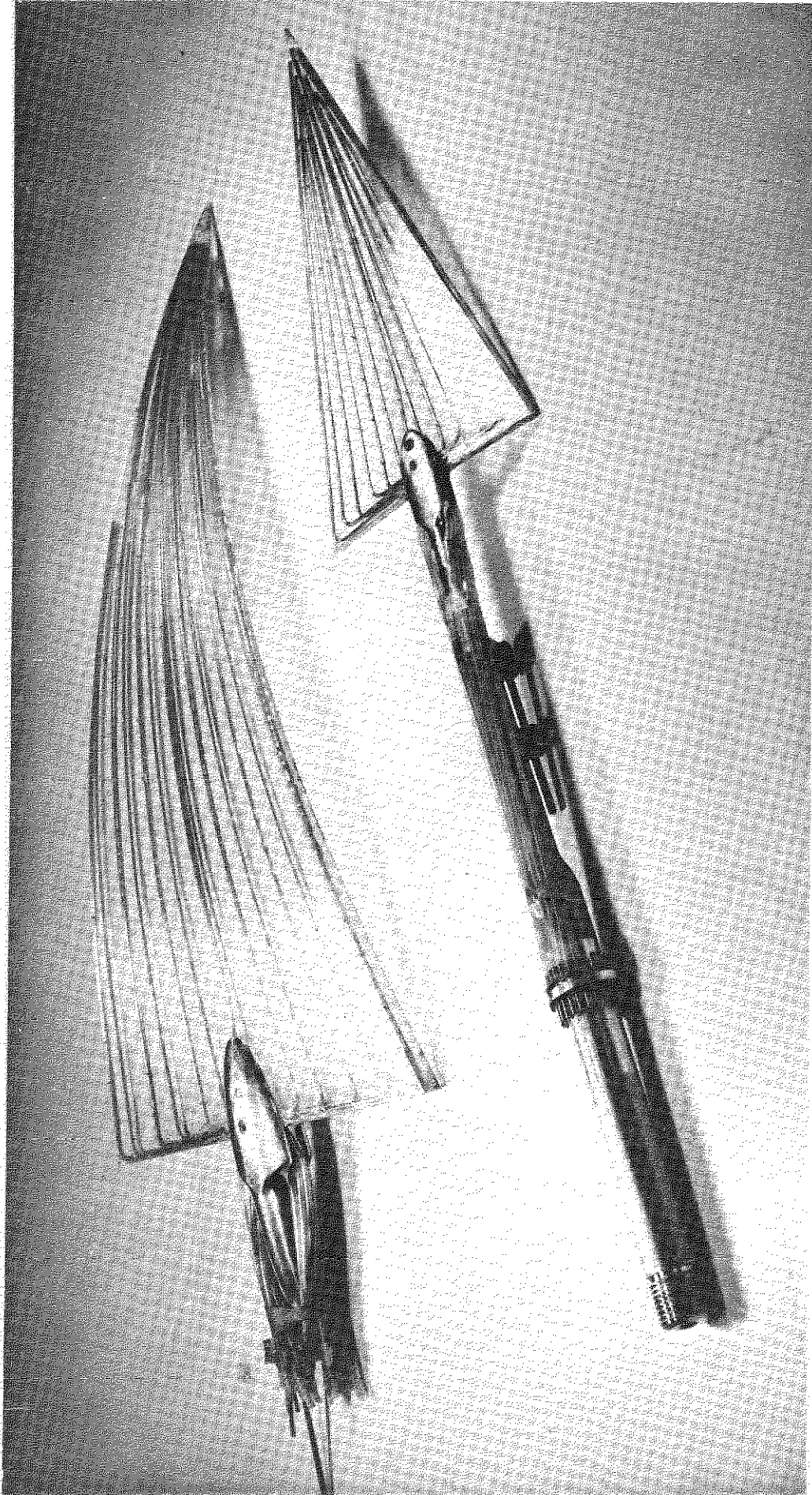
Comparison of the experimental streamwise lift distribution with Taylor's linear theory seems to be extremely good. Obviously Taylor's cannot predict the small change of the centre of pressure of an uncambered wing with leading edge separation with increasing incidence, but the theory seems to give a good first approximation to the changes in centre of pressure due to camber effects.

It is of interest to relate the present results to the ideas of Polhamus. He has shown that C_L for delta wings with leading edge separation can be given closely from linear theory by assuming that in addition to the linear lift the effect of the leading edge separation is to rotate the linearised leading edge thrust through 90° to act as the incremental non-linear lift. Presumably linear theory for slender wings gives a streamwise distribution of leading edge thrust which is similar to the streamwise linear lift distribution, so that according to Polhamus we might expect a close similarity between the linear and non-linear streamwise lift distributions shown up in this note. Tentatively it seems at this stage that the Polhamus concept might be extended to give the centre of pressure of a slender wing in addition to its non-linear C_L . Spanwise loadings, however, are not predicted by any of these methods.

REFERENCES

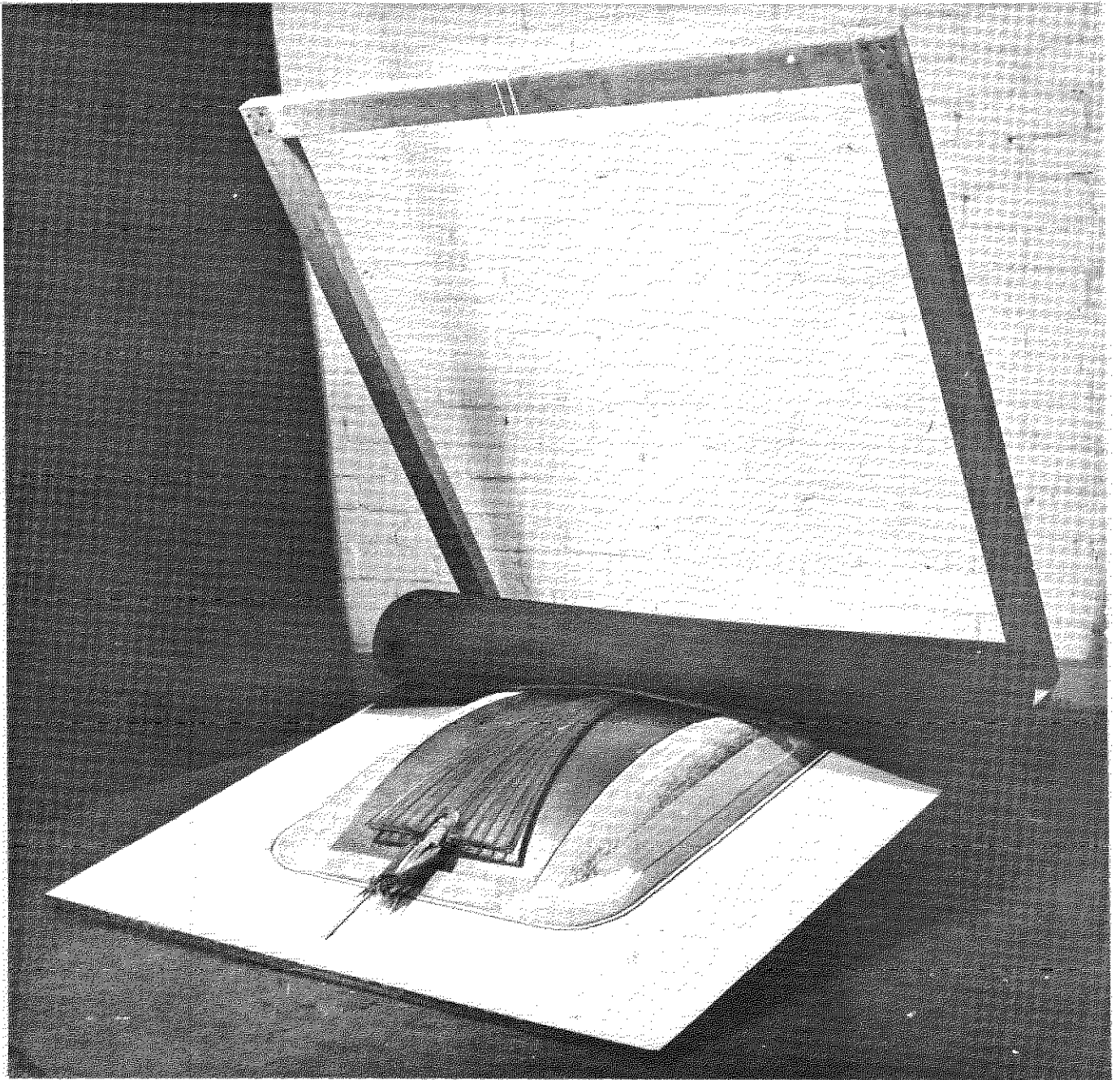
1. G.J. Hancock The Static Aeroelasticity of Slender Configurations. Parts I - IV, Aero. Quart. 1961-3.
 2. R.D. Milne The Dynamics of the Deformable Aeroplane. A.R.C. R.& M.3345 (1962).
 3. R.K. Nangia The Effects of Longitudinal Camber on Slender Wings. Ph.D. Thesis, University of London, June, 1967.
 4. R.K. Nangia and A Theoretical Investigation for Delta Wings with Leading Edge Separation at Low Speeds. G.J. Hancock A.R.C.30 608 - F.M.3994, August 1968.
 5. J. Black An Experimental Investigation of the Effects of Deformation on the Aerodynamic Characteristics of a Swept Back Wing. A.R.C. R.& M.2938, 1953.
 6. C.R. Taylor A Subsonic Lifting Surface Theory for Low Aspect Ratio Wings. A.R.C. R.& M.3051, 1956.
 7. E.C. Polhamus A Concept of the Vortex Lift of Sharp Edge Delta Wings based on a Leading Edge Suction Analogy. NASA TN D-3767, 1966.
-

FIG. 1(a)

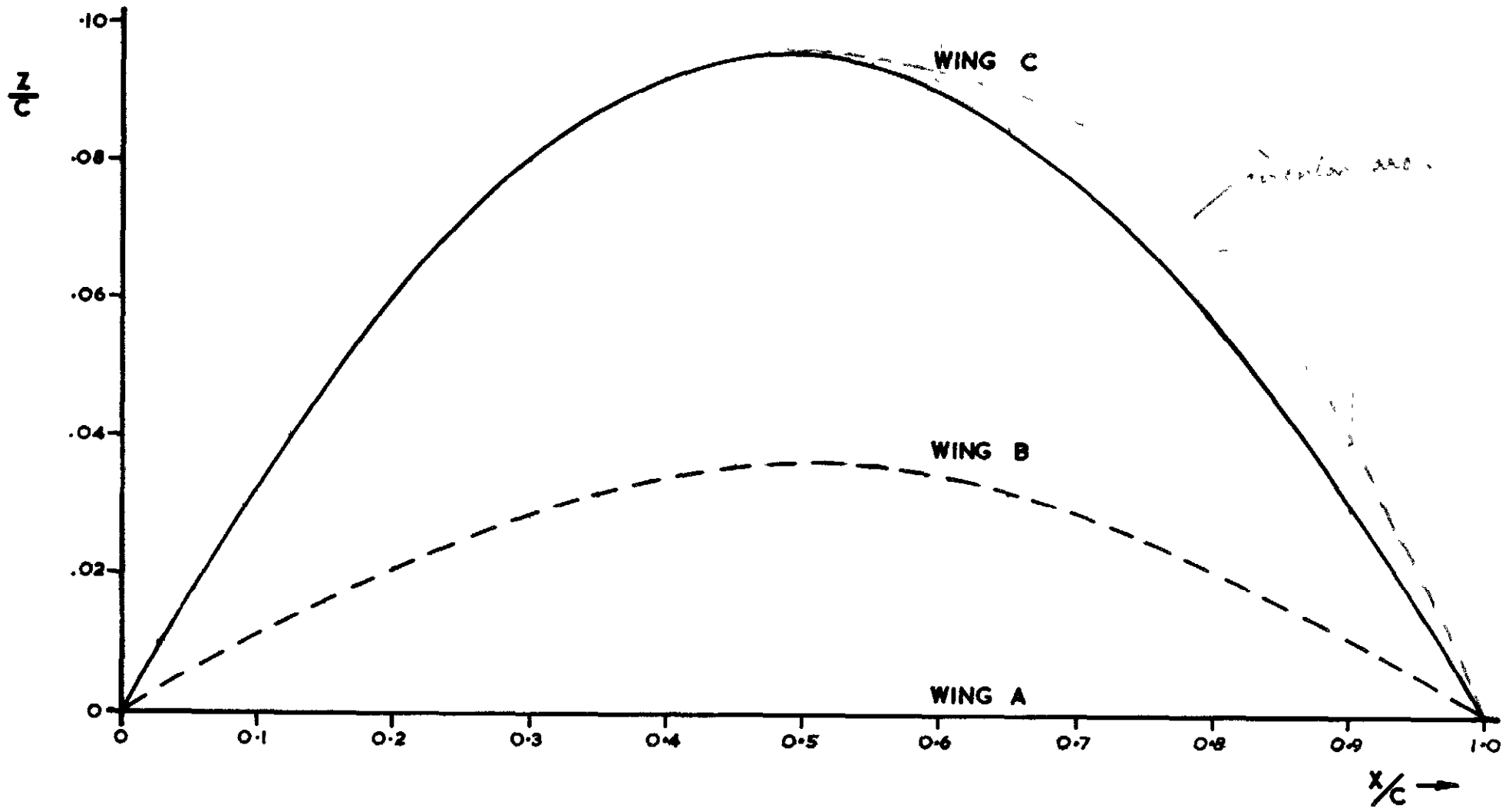


Wing models

FIG.1 (b)

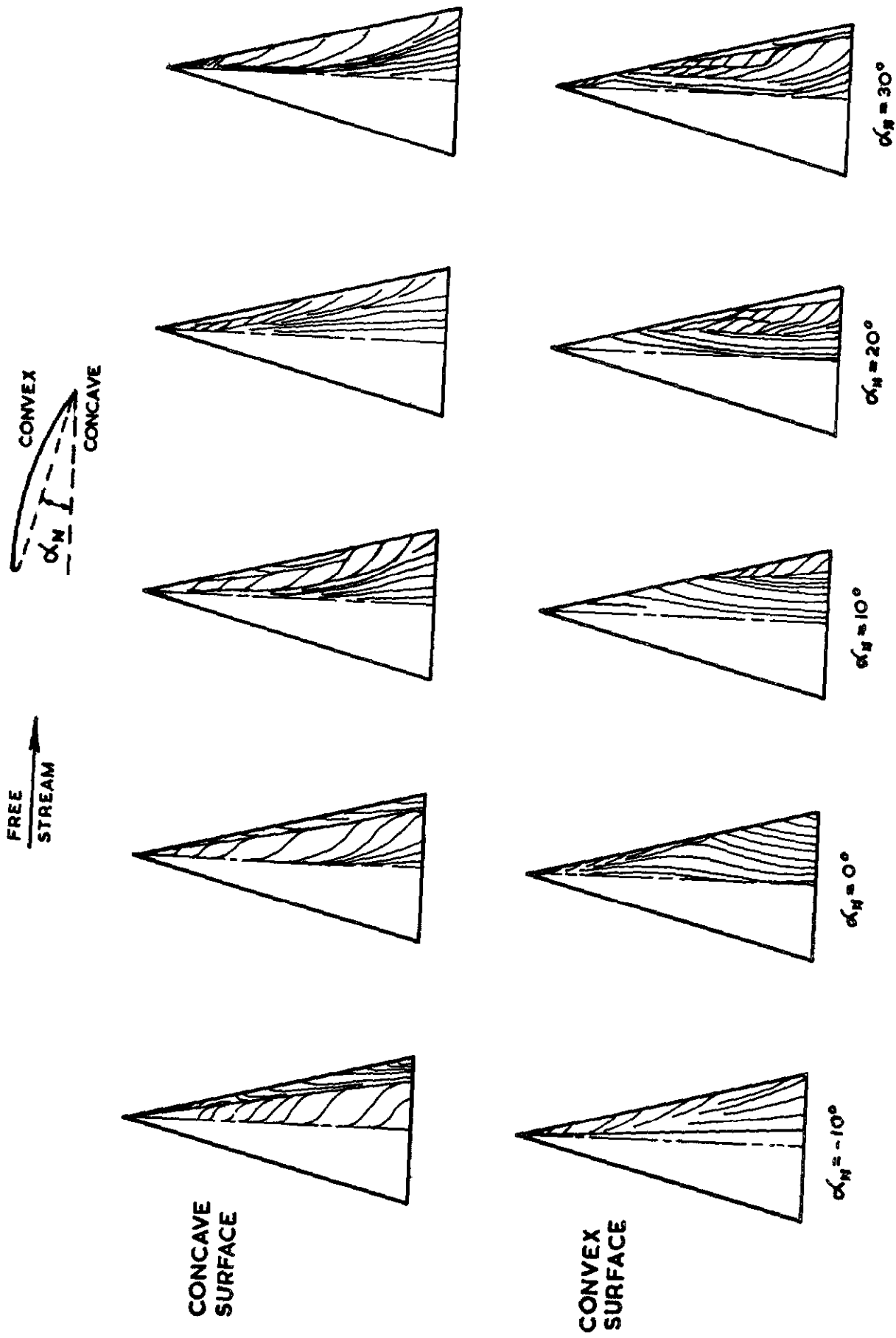


Wing mould apparatus

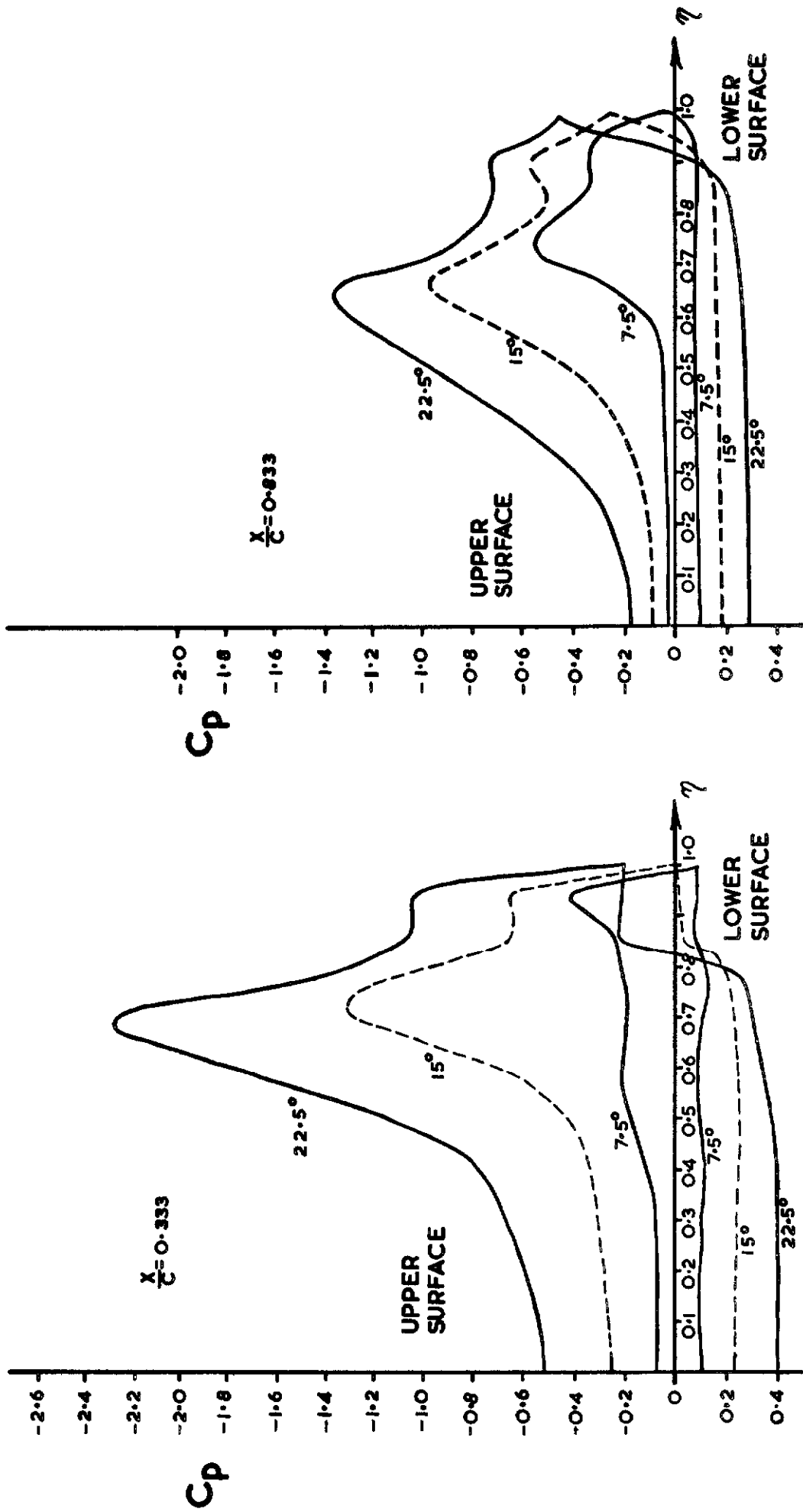


CHORDWISE CAMBER MODES FOR WINGS B & C

Fig. 2

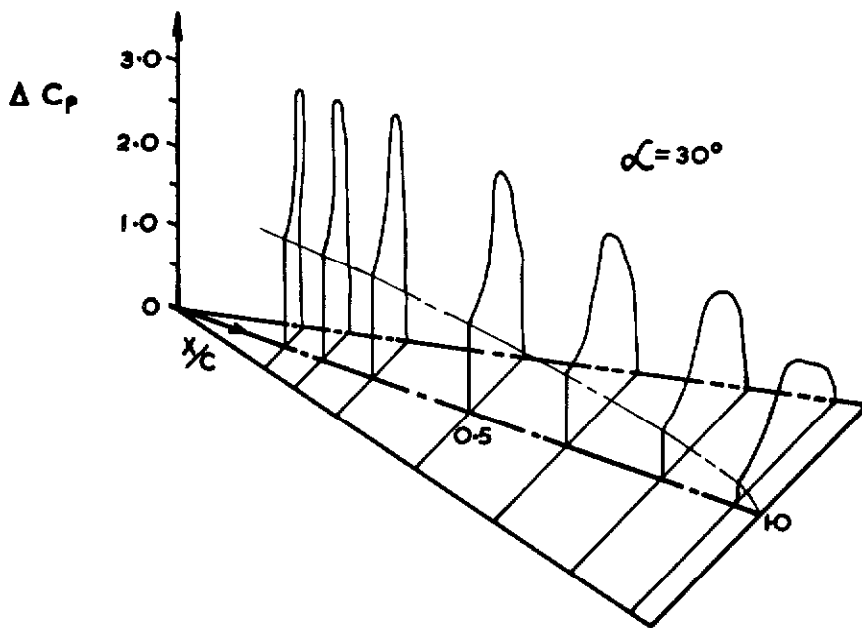
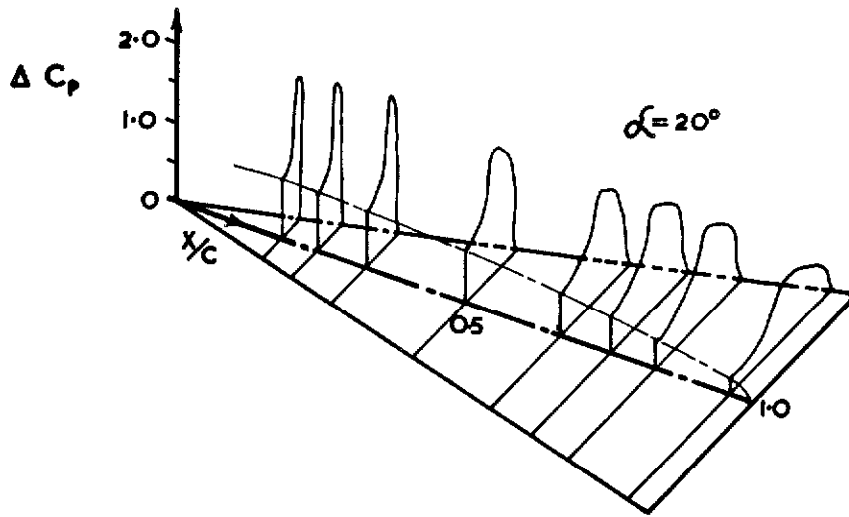
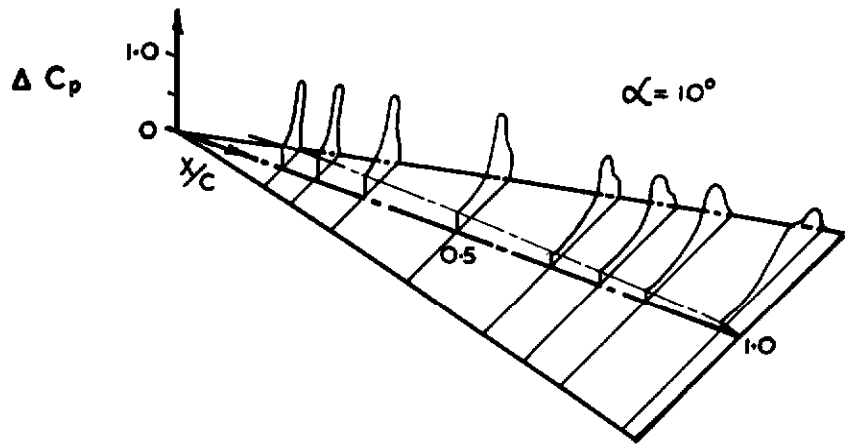


FLOW PATTERNS ON WING C (9.46% camber)
 Fig. 3



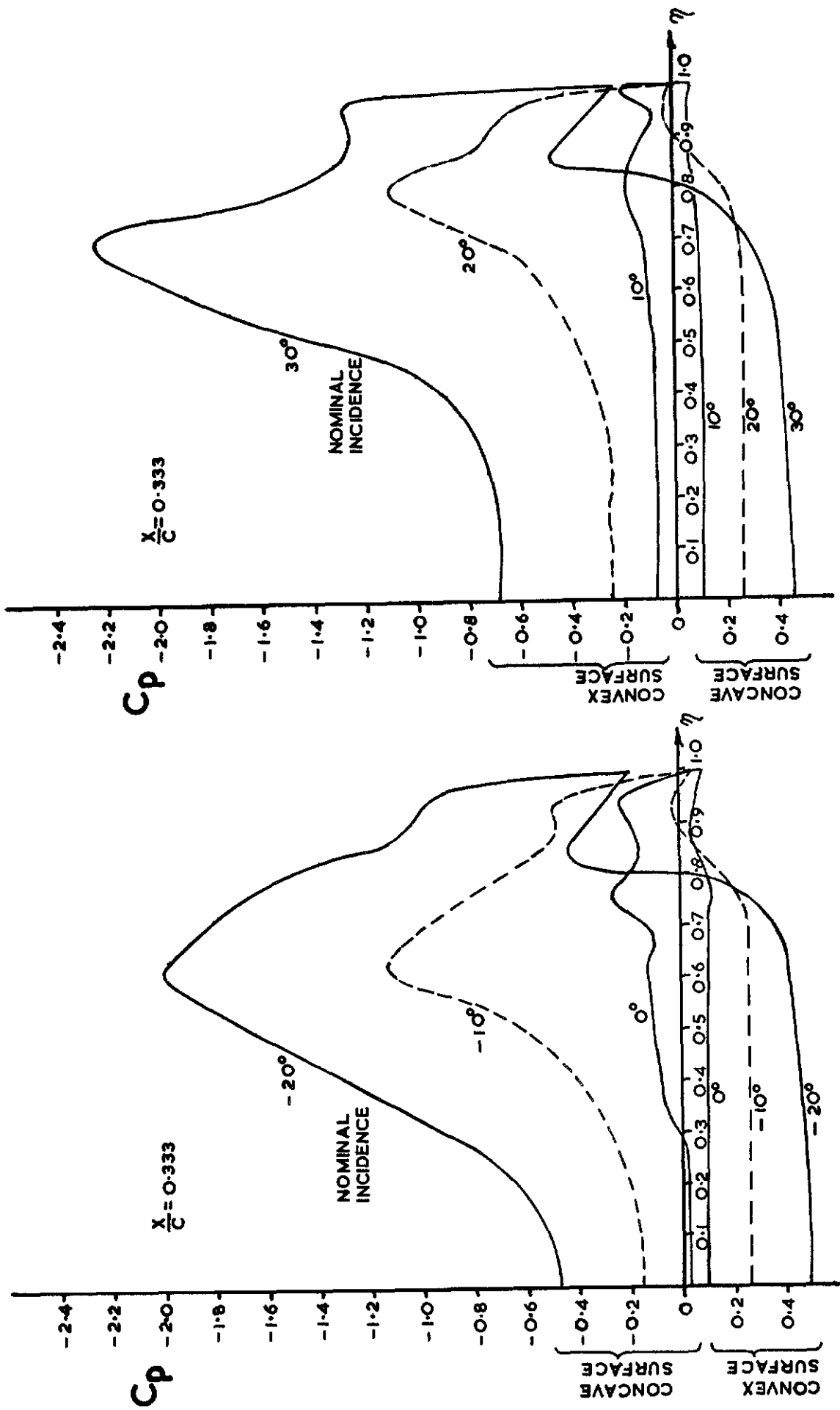
PRESSURE COEFFICIENTS ON UPPER AND LOWER SURFACES FOR WING A AT TWO CHORDWISE STATIONS

Fig. 4



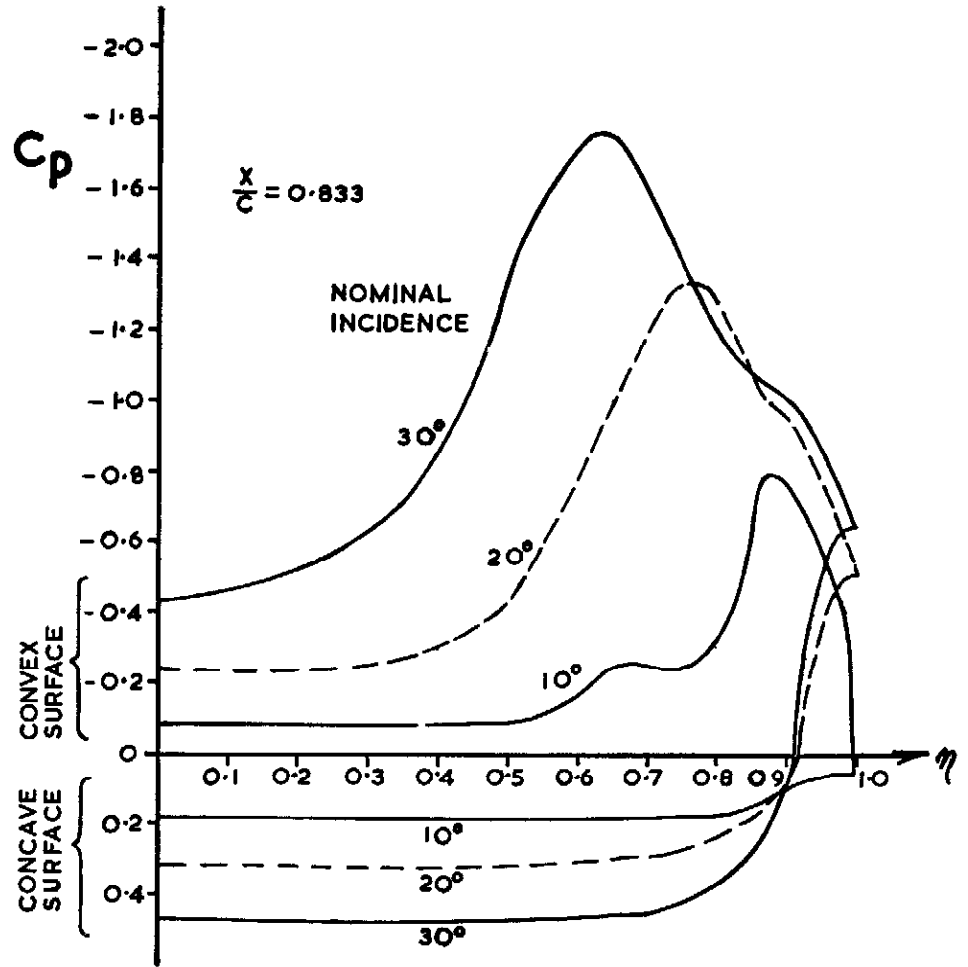
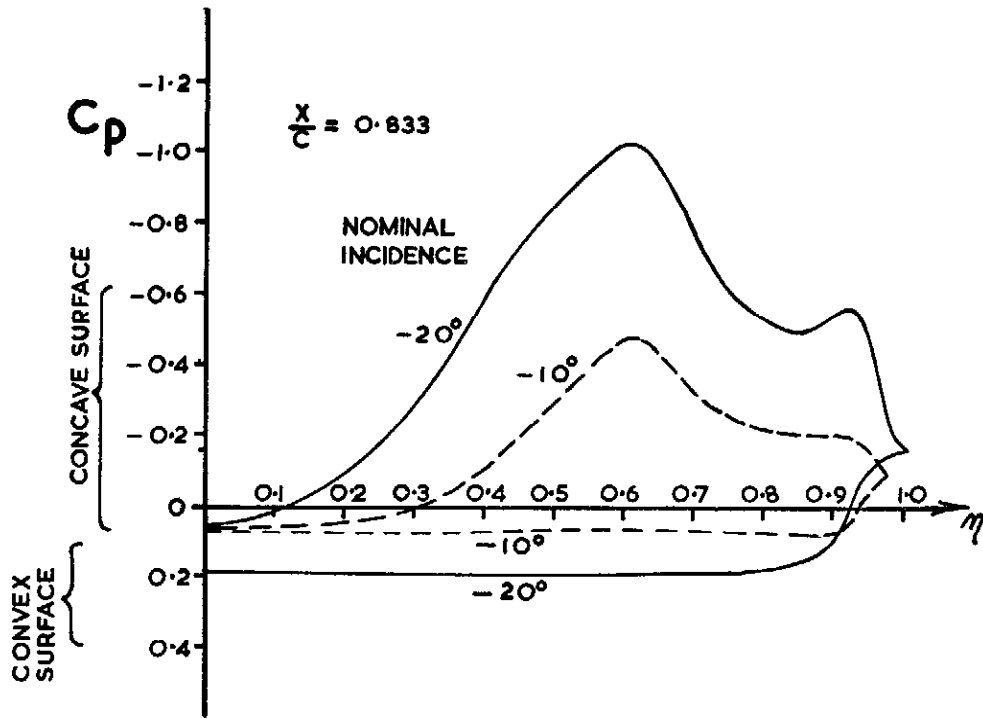
SKETCH OF LOAD DISTRIBUTION ON UNCAMBERED WING

Fig. 5



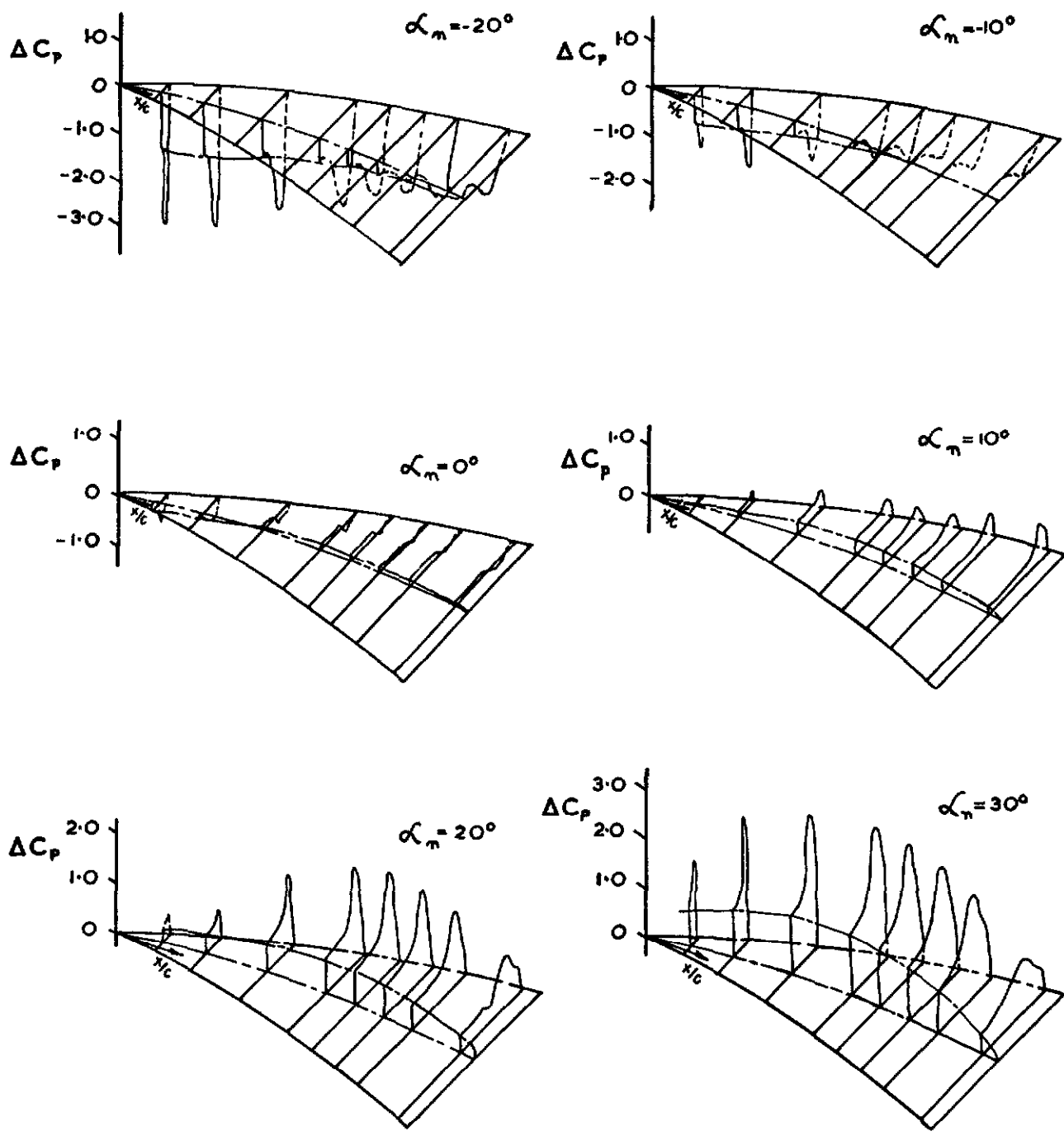
PRESSURE COEFFICIENTS FOR WING B AT $X/C = 0.333$

Fig. 6 a.



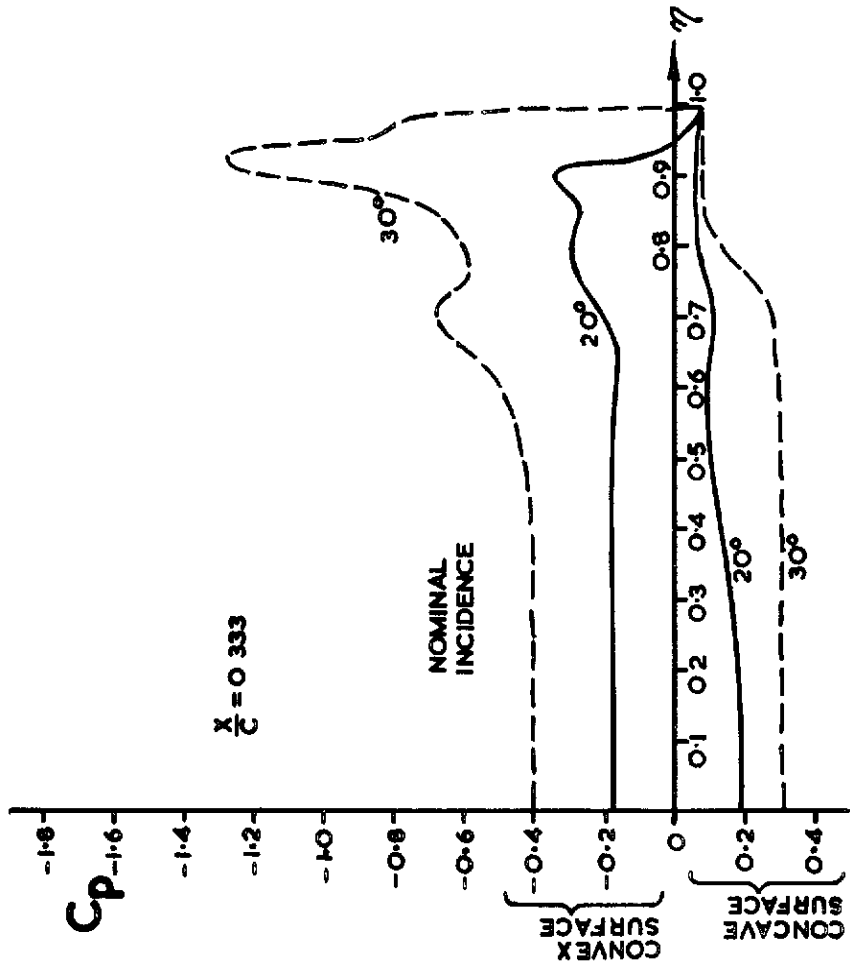
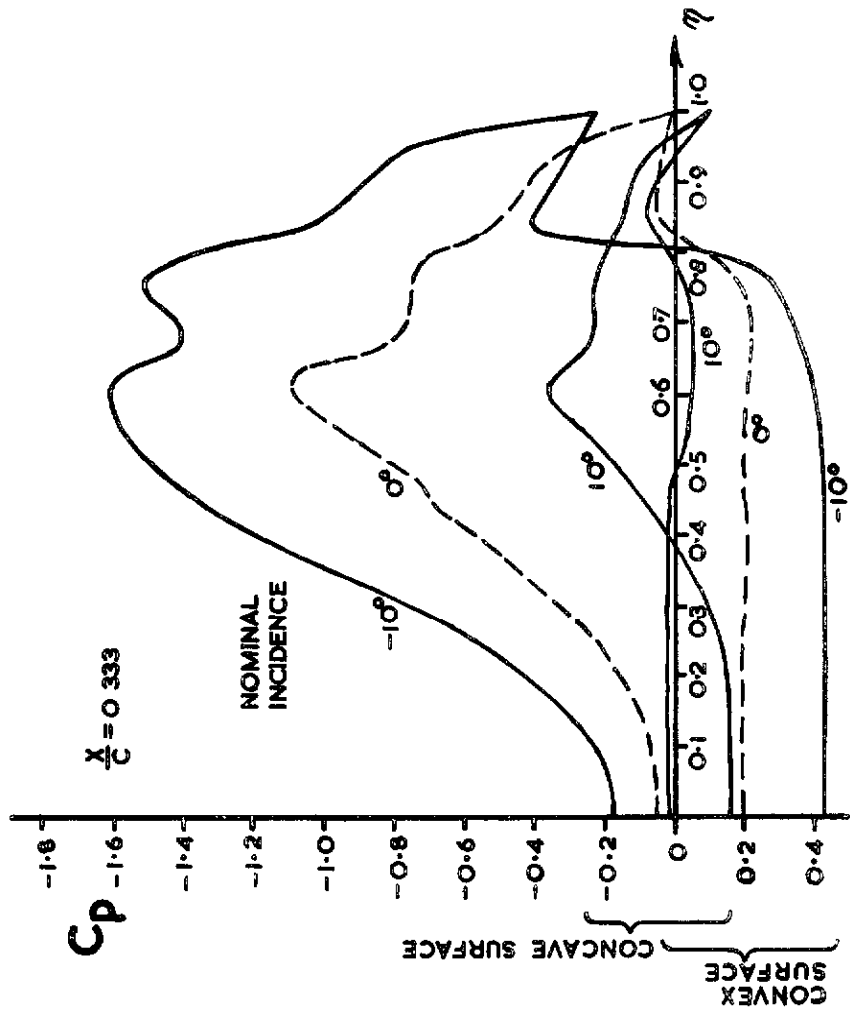
PRESSURE COEFFICIENTS FOR WING B AT $x/c = 0.833$

Fig. 6 b



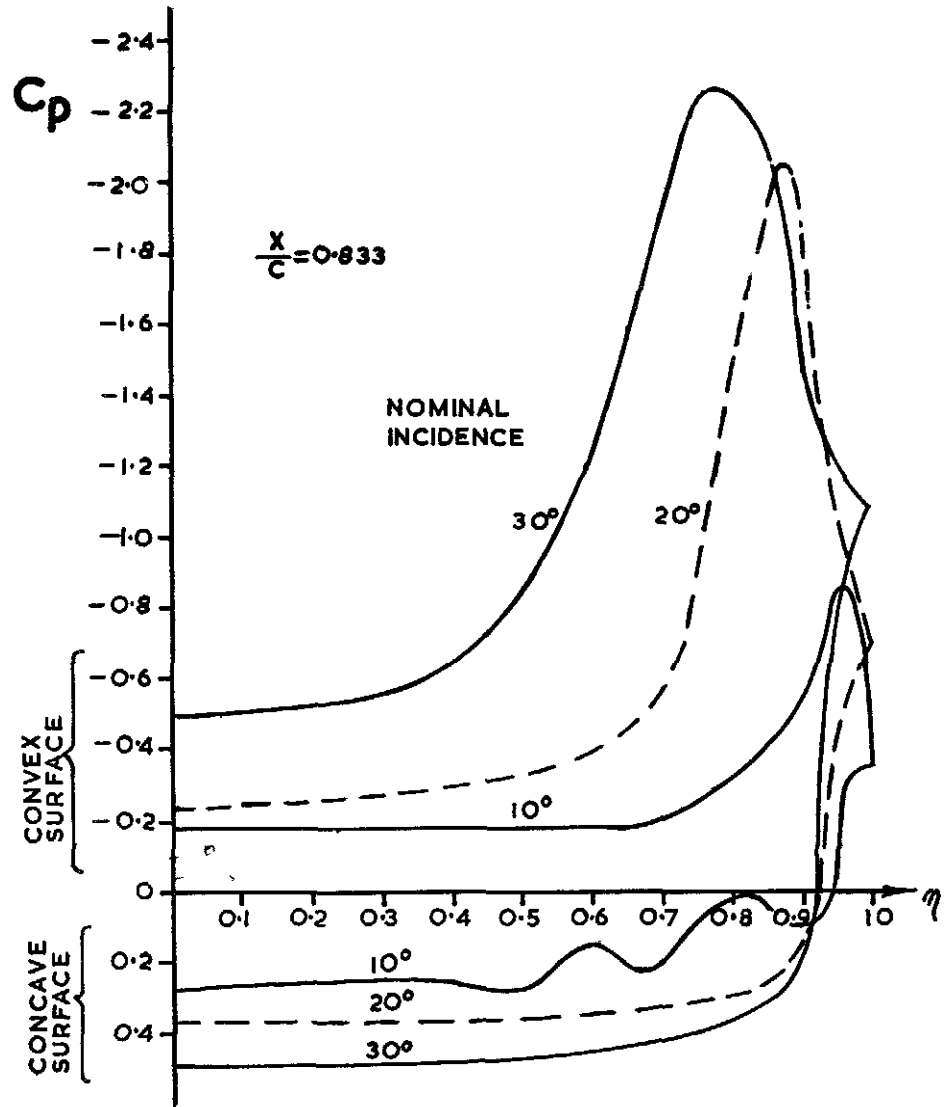
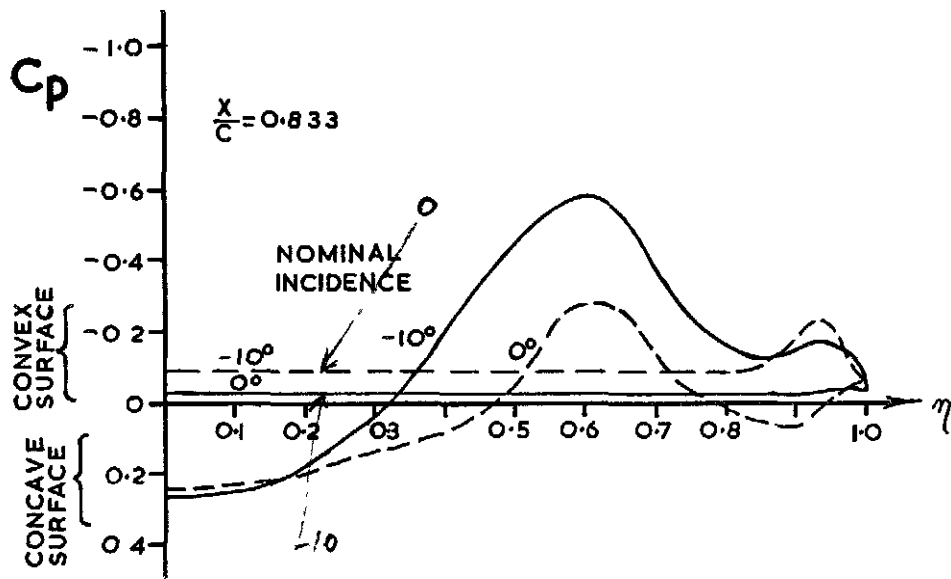
SKETCH OF LOAD DISTRIBUTIONS FOR CAMBERED WING B

Fig. 7



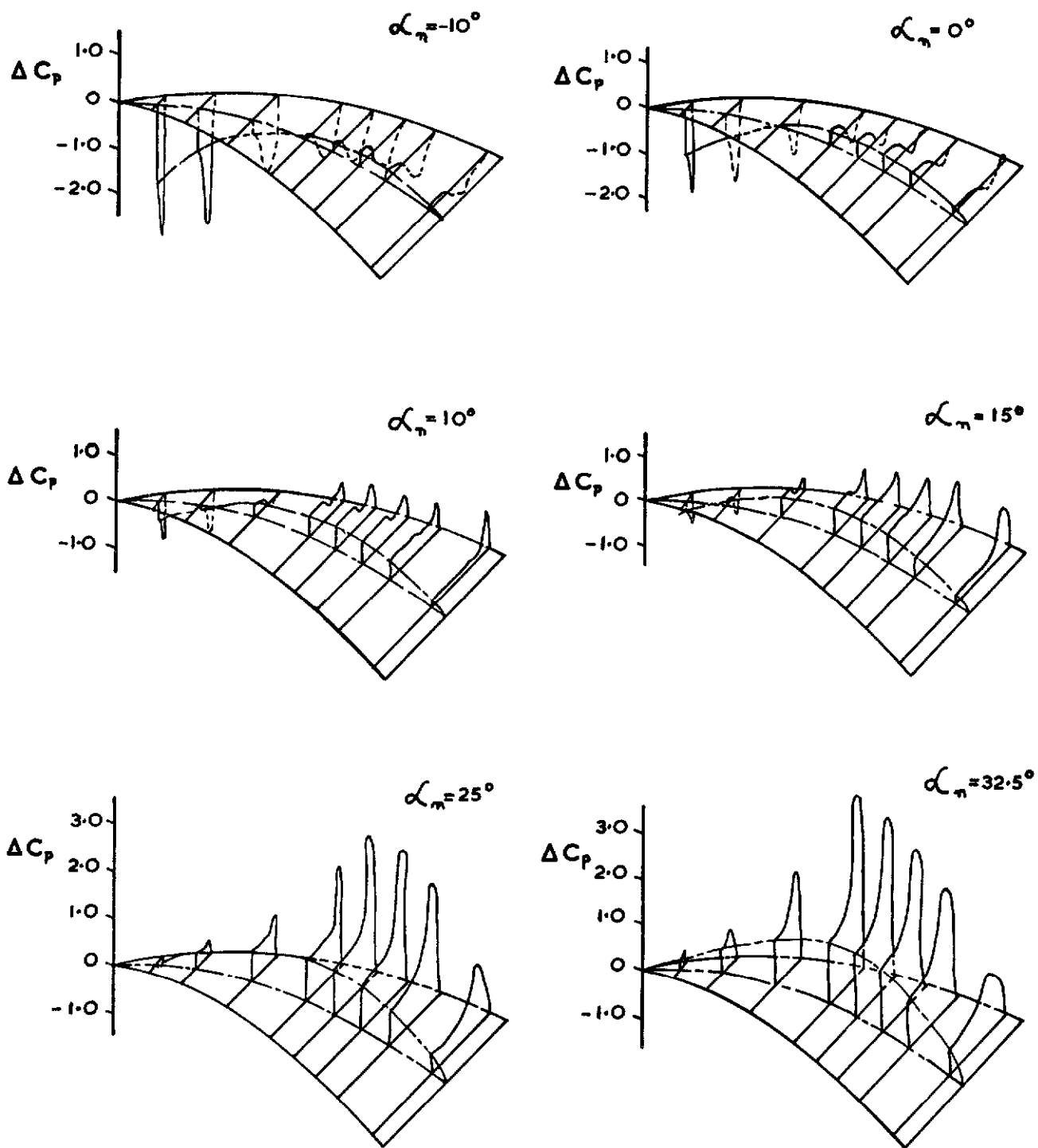
PRESSURE COEFFICIENTS FOR WING C AT $\frac{x}{c} = 0.333$

Fig. 8a.



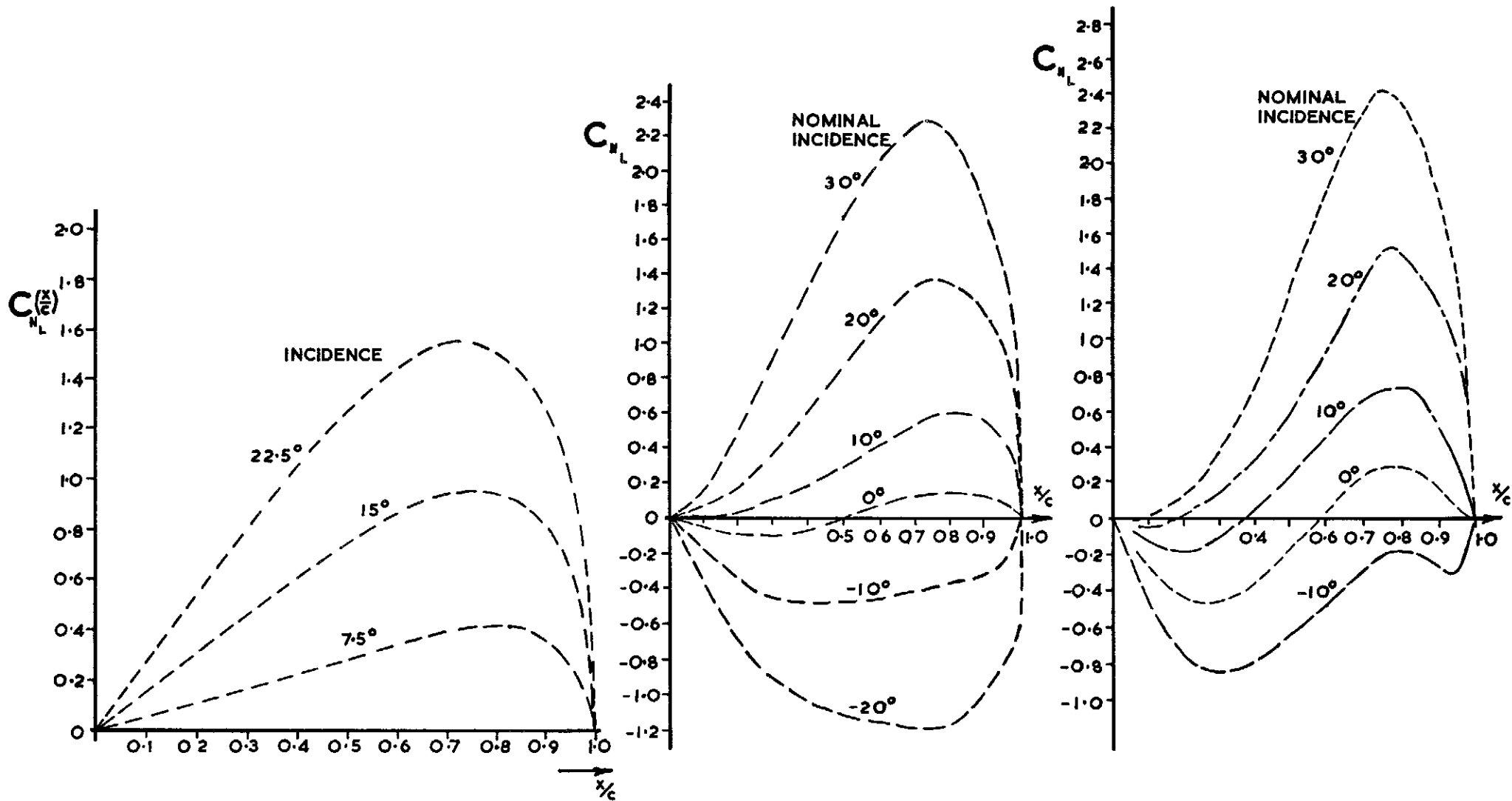
PRESSURE COEFFICIENTS FOR WING C AT $x/c = 0.833$

Fig. 8 b.



SKETCH OF LOAD DISTRIBUTIONS FOR WING C

Fig. 9



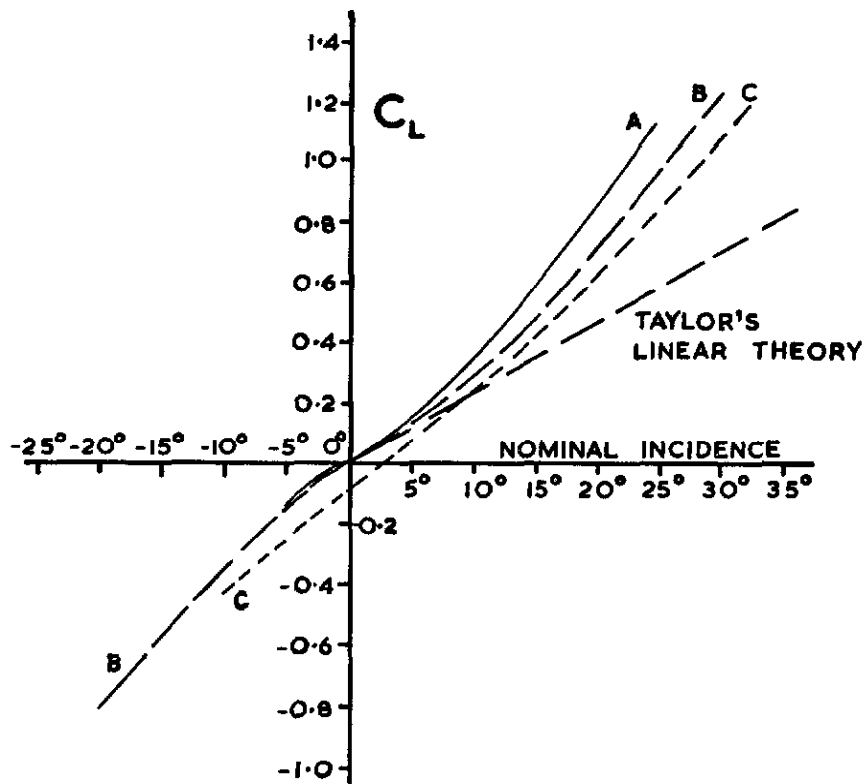
UNCAMBERED WING A

CAMBERED (3.57%) WING B

CAMBERED (9.46%) WING C

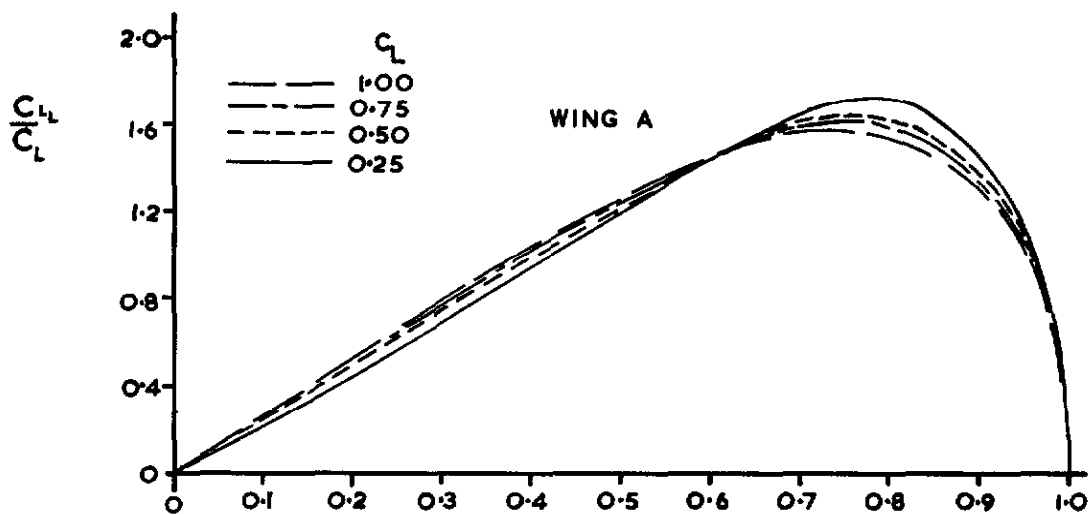
LONGITUDINAL DISTRIBUTION OF LOCAL NORMAL FORCE COEFFICIENTS

Fig. 10



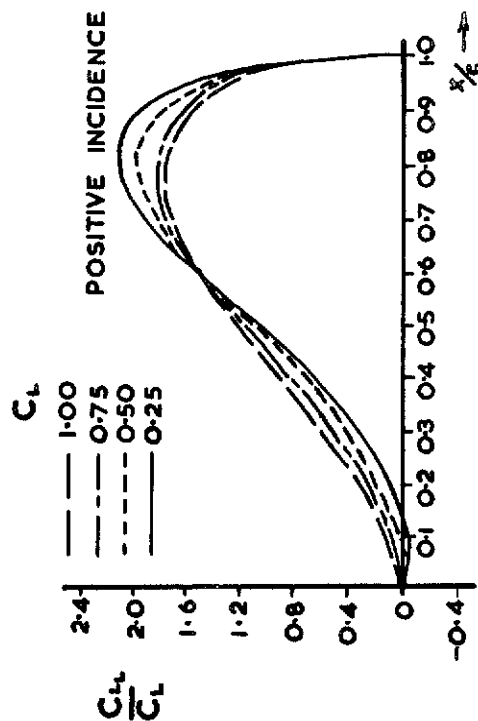
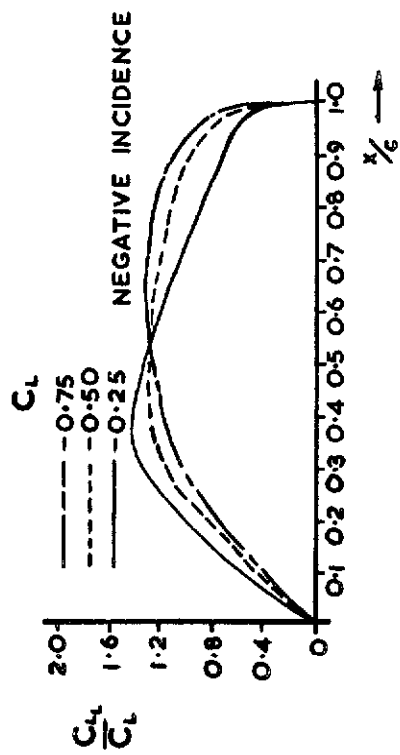
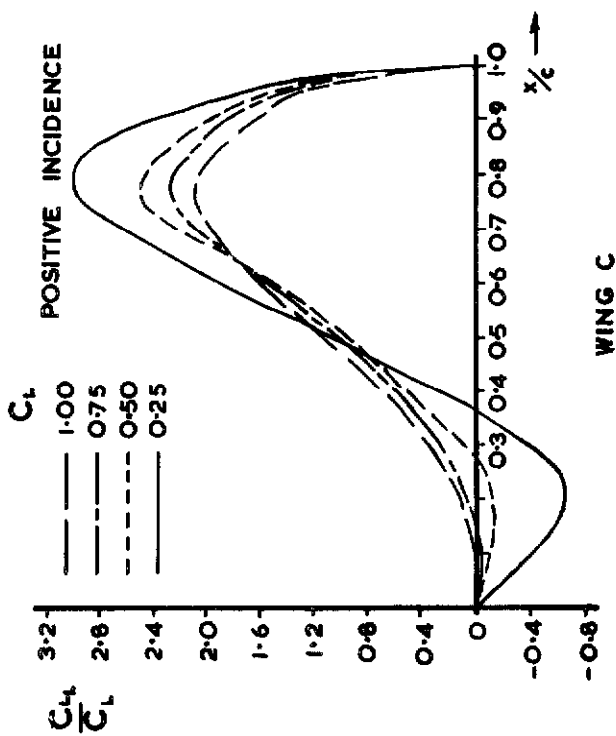
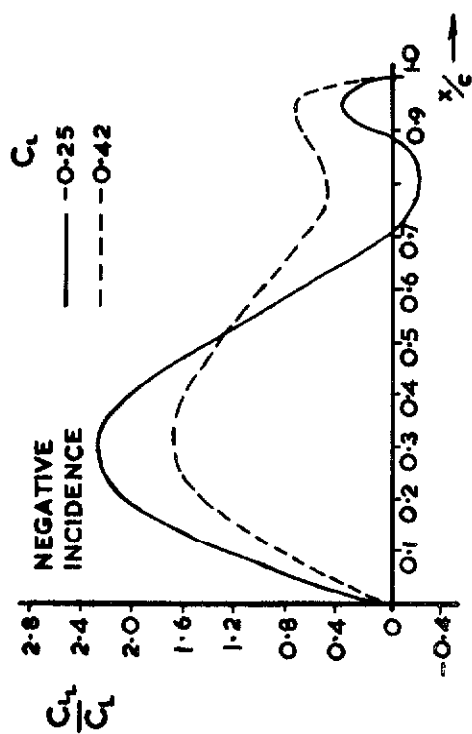
VARIATION OF LIFT COEFFICIENT WITH NOMINAL INCIDENCE FOR WINGS A, B, C

Fig. 11



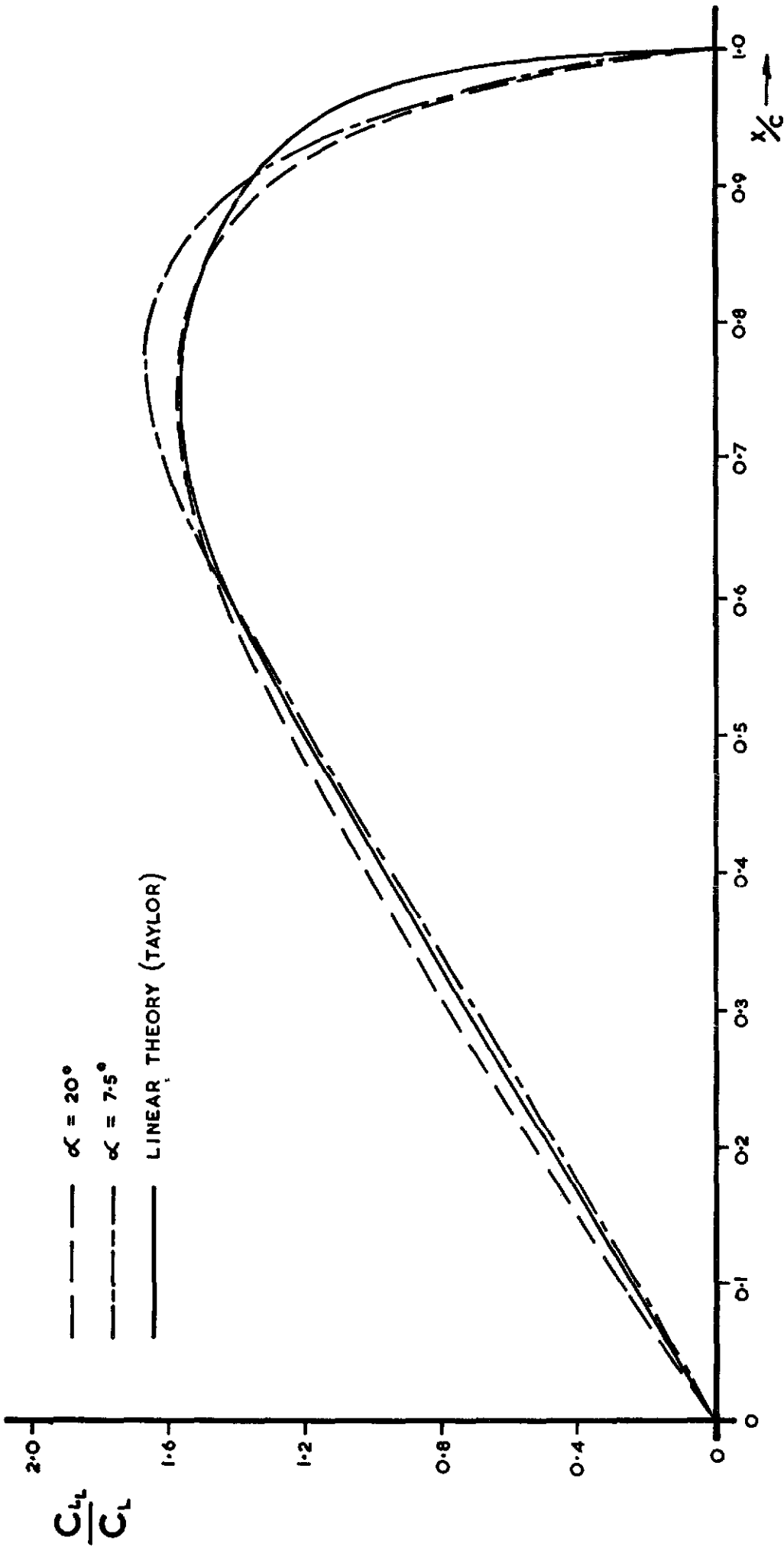
LIFT DISTRIBUTION ON UNCAMBERED WING A

Fig. 12



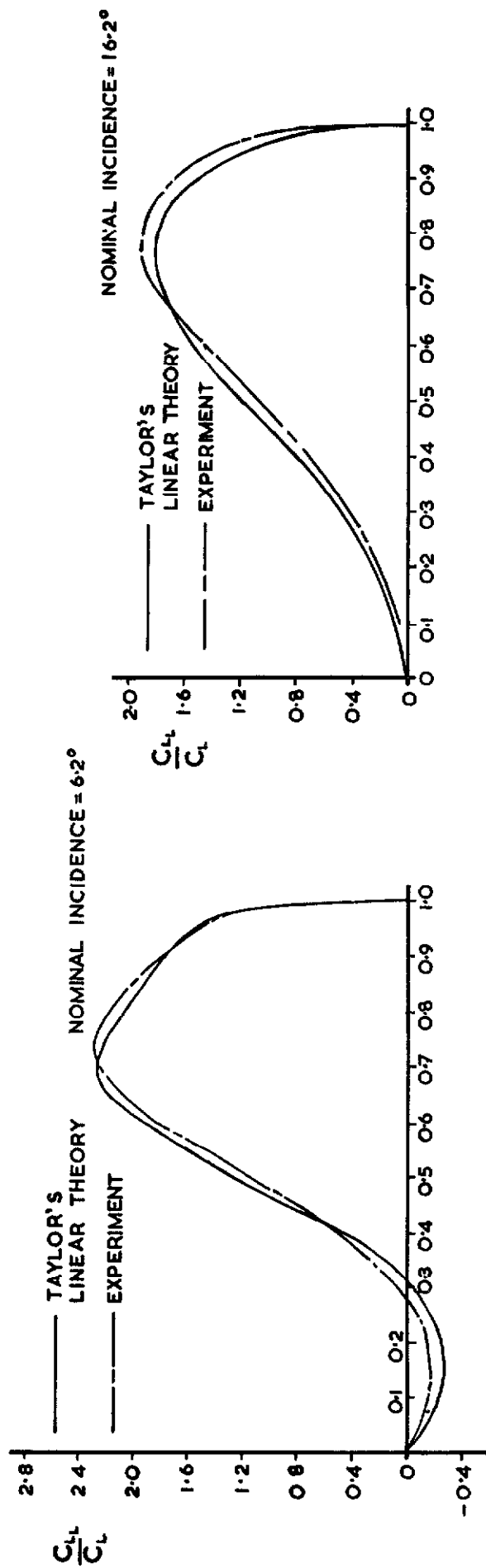
LONGITUDINAL DISTRIBUTION AT VARIOUS LIFT COEFFICIENTS FOR CHORDWISE CAMBERED WINGS B AND C

Fig. 13



COMPARISON OF THEORY AND EXPERIMENT FOR UNCAMBERED WING

Fig. 14



COMPARISON OF LONGITUDINAL DISTRIBUTIONS FOR WING B

Fig. 15

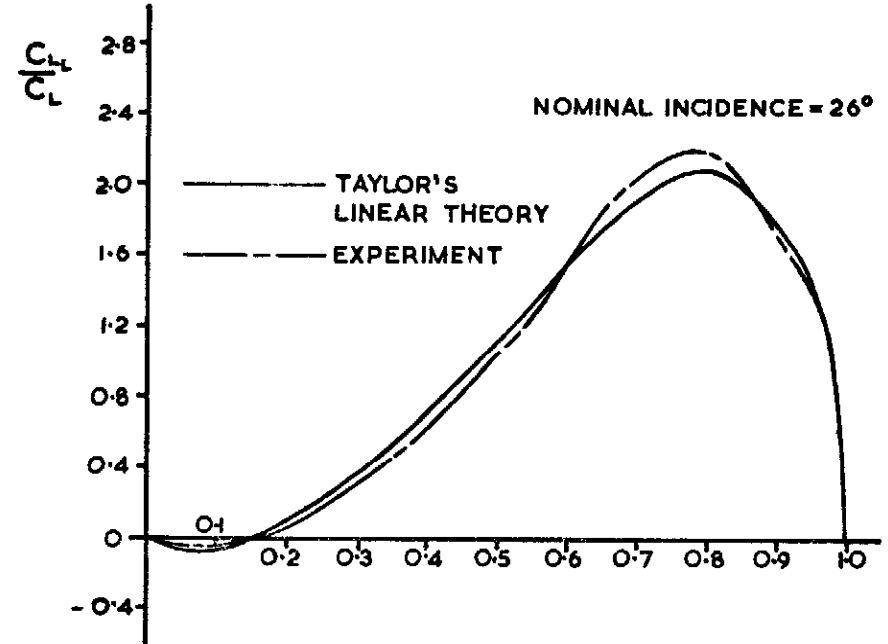
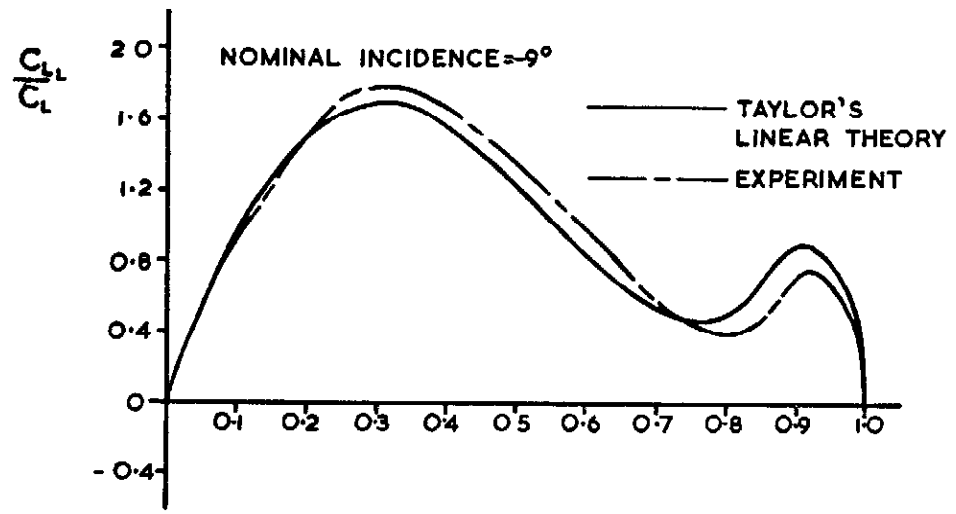
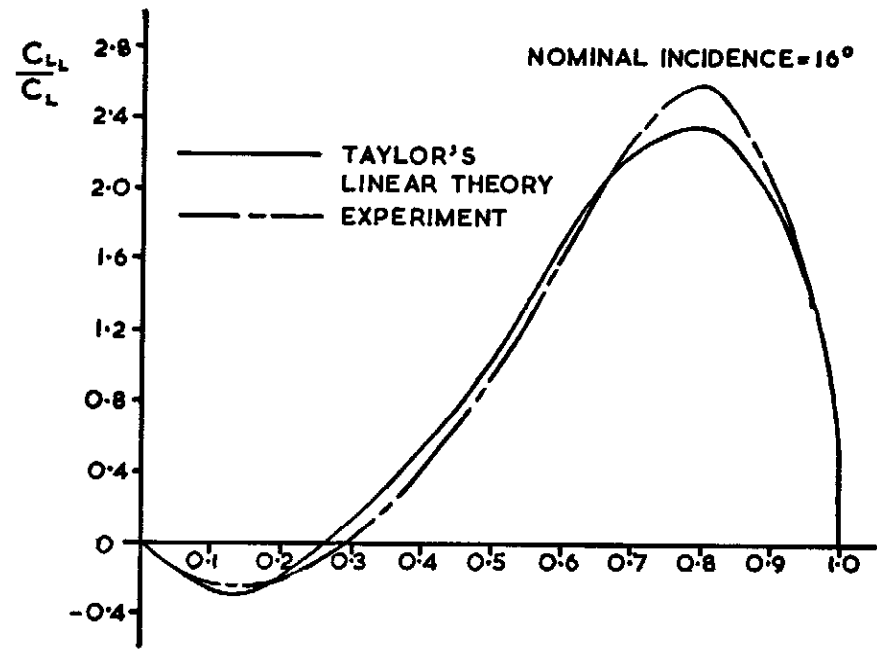
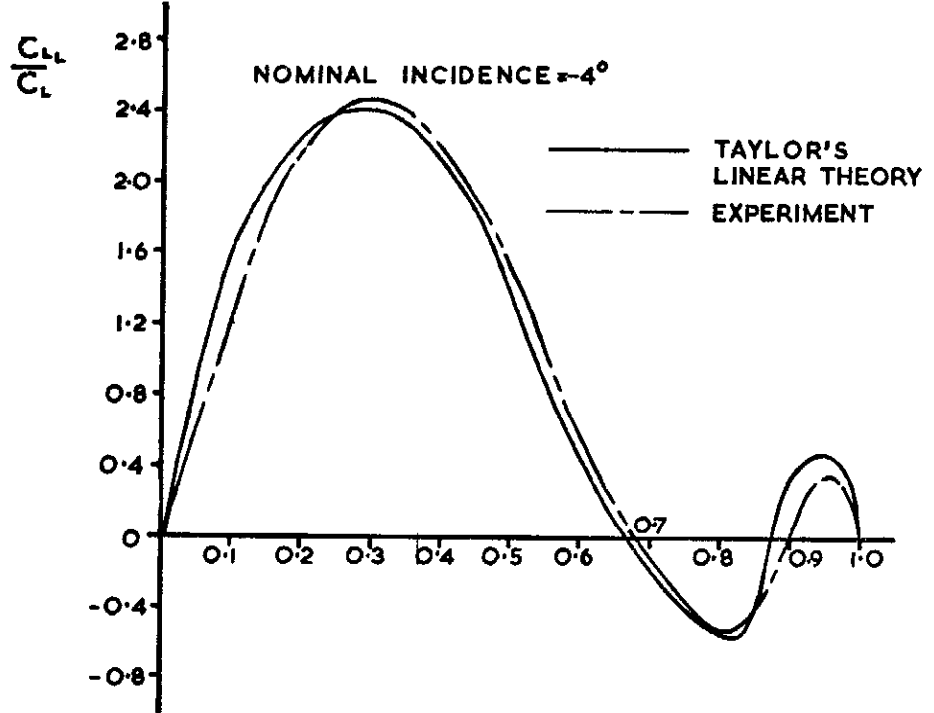


Fig.16 COMPARISON OF LONGITUDINAL DISTRIBUTIONS FOR WING C

A.R.C. C.P. No.1129
September 1969

Nangia, R. K.
Hancock, G. J.

DELTA WINGS WITH LONGITUDINAL CAMBER AT LOW SPEED

Experiments on a delta wing of aspect ratio 1 with various streamwise cambers are reported. Comparison of experimental results for the streamwise lift distribution with Taylor's simplified slender linear theory is remarkably good even for large cambers, although linear theory is totally inadequate for total lift prediction. The good agreement between experiment and linear theory for the streamwise lift distribution indicates support for the recent intuitive ideas of Polhamus.

A.R.C. C.P. No.1129
September 1969

Nangia, R. K.
Hancock, G. J.

DELTA WINGS WITH LONGITUDINAL CAMBER AT LOW SPEED

Experiments on a delta wing of aspect ratio 1 with various streamwise cambers are reported. Comparison of experimental results for the streamwise lift distribution with Taylor's simplified slender linear theory is remarkably good even for large cambers, although linear theory is totally inadequate for total lift prediction. The good agreement between experiment and linear theory for the streamwise lift distribution indicates support for the recent intuitive ideas of Polhamus.

A.R.C. C.P. No.1129
September 1969

Nangia, R. K.
Hancock, G. J.

DELTA WINGS WITH LONGITUDINAL CAMBER AT LOW SPEED

Experiments on a delta wing of aspect ratio 1 with various streamwise cambers are reported. Comparison of experimental results for the streamwise lift distribution with Taylor's simplified slender linear theory is remarkably good even for large cambers, although linear theory is totally inadequate for total lift prediction. The good agreement between experiment and linear theory for the streamwise lift distribution indicates support for the recent intuitive ideas of Polhamus.

© *Crown copyright 1970*

Printed and published by
HER MAJESTY'S STATIONERY OFFICE

To be purchased from
49 High Holborn, London WC1
13a Castle Street, Edinburgh EH2 3AR
109 St Mary Street, Cardiff CF1 1JW
Brazennose Street, Manchester M60 8AS
50 Fairfax Street, Bristol BS1 3DE
258 Broad Street, Birmingham 1
7 Linenhall Street, Belfast BT2 8AY
or through any bookseller

Printed in England